

Article

Piezoresistive Chemical Sensors Based on Functionalized Hydrogels

Margarita Guenther ^{1,2,*}, Thomas Wallmersperger ² and Gerald Gerlach ¹

¹ Solid-State Electronics Lab, Technische Universität Dresden, Helmholtzstr. 18, Dresden 01062, Germany; E-Mail: Gerald.Gerlach@tu-dresden.de

² Institute of Solid Mechanics, Technische Universität Dresden, George-Bähr-Str. 3c, Dresden 01062, Germany; E-Mail: thomas.wallmersperger@tu-dresden.de

* Author to whom correspondence should be addressed; E-Mail: mguenthe@mail.zih.tu-dresden.de; Tel.: +49-351-4633-5378; Fax: +49-351-4633-2320.

Received: 3 July 2013; in revised form: 15 April 2014 / Accepted: 14 May 2014 /

Published: 10 June 2014

Abstract: Thin films of analyte-specific hydrogels were combined with microfabricated piezoresistive pressure transducers to obtain chemomechanical sensors that can serve as selective biochemical sensors for a continuous monitoring of metabolites. The gel swelling pressure has been monitored in simulated physiological solutions by means of the output signal of piezoresistive sensors. The interference by fructose, human serum albumin, pH, and ionic concentration on glucose sensing was studied. With the help of a database containing the calibration curves of the hydrogel-based sensors at different values of pH and ionic strength, the corrected values of pH and glucose concentration were determined using a novel calibration algorithm.

Keywords: polyelectrolyte hydrogel; analyte-specific swelling behavior; piezoresistive microsensor; chemical sensor

1. Introduction

Hydrogels are three-dimensionally cross-linked hydrophilic polymer networks swollen in water which are able to undergo a volume phase transition under the influence of environmental changes. The amount of solvent uptake depends on the polymer structure and composition, and can be made

particularly responsive to environmental factors, such as temperature, pH-value, ion concentration, salt concentration, analyte molecule concentration in solutions, and solvent composition.

The ability to customize the hydrogels' chemical and mechanical characteristics allows for the synthesis of hydrogels optimized for detection of particular target species in a physiological concentration range. In the presence of an analyte, these polymers alter their swelling properties, either by ionization or by formation of analyte-mediated reversible crosslinks [1–5].

The diagnosis and management of metabolic diseases, such as diabetes mellitus, requires a simultaneous and continuous monitoring of several metabolites (blood glucose level, pH-value, concentration of CO₂) throughout day with the help of measuring systems. In this regard, a new challenge is an implantable sensor array microsystem consisting of several hydrogel-based sensors that can provide a continuous monitoring and on-line control of physiological parameters in the body fluid. Glucose levels in interstitial fluid lag temporally (*ca.* 5 min) behind blood glucose values [6–8]. Diabetes mellitus results from insulin deficiency and hyperglycemia, and is reflected by blood glucose concentrations higher or lower than the normal range of 4.4–6.6 mM (80–120 mg/dL). To account for both physiological (normoglycemia) and pathophysiological (hypo- and hyperglycemia) ranges, sensors should measure between 1 and 22 mM (18–400 mg/dL) with a response time not greater than 7 min to reach 90% of steady state [7].

Hydrogel-based sensors generally consist of two main components, the polymeric hydrogel used for the biochemical detection and a transducer. Transducers involving mechanical [3,9–15], electrochemical (e.g., capacitive [2], conductometric, amperometric, potentiometric [16]), and optical [17] mechanisms are used to monitor changes in hydrogel volume and structure. The pH-, ionic strength- and glucose-sensitive hydrogels undergo reversible volume transitions with environmental changes. These volume transitions produce swelling pressures, which are the basis for the chemical-mechanical transduction of piezoresistive hydrogel-based sensors [3,9–12]. Hydrogels can readily be miniaturized and directly integrated into piezoresistive pressure sensors. Moreover, hydrogels with various moieties can be used simultaneously in sensor arrays to detect a number of physiological analytes (e.g., glucose, pH, CO₂, ionic strength) [18,19]. In this context, it is important to estimate the gel swelling pressure due to the concentration variation of metabolites in complex physiological solutions and to validate the performance of piezoresistive chemomechanical sensors operating on the basis of this pressure.

In general, two components of the hydrogel control its swelling response, the chemical nature of polymer chains that make up the network and their compatibility with water, and the nature and amount of crosslinking species. Additionally, for hydrogels containing fixed ionizable groups, a third ionic component, which depends on the degree of ionization, affects the swelling process.

Flory-Rehner-Donnan-Tanaka theory, which takes into consideration these three effects, has been used classically to explain the swelling behavior of hydrogels [20–24]. According to this theory, the swelling state of the hydrogel network is associated with the sum of three swelling pressures $\Delta\pi_{\text{mixing}}$, $\Delta\pi_{\text{elastic}}$, and $\Delta\pi_{\text{ionic}}$, which sum to zero under thermodynamic equilibrium conditions (see Equation (A1) in Appendix A). For a nonionic hydrophilic hydrogel, the mixing of water with the polymer makes a negative contribution $\Delta\pi_{\text{mixing}}$, while the stretching of the hydrogel network yields a positive contribution $\Delta\pi_{\text{elastic}}$. For a polyelectrolyte hydrogel, there is an additional negative contribution $\Delta\pi_{\text{ionic}}$ associated with the mixing of water with the counterions. Ionic osmotic pressure $\Delta\pi_{\text{ionic}}$, the third force dictating the swelling behavior of the hydrogel, is observed only in hydrogels bearing fixed charges on

the polymer chains. These fixed charges must be electrically compensated by mobile counterions, which exert the swelling pressure on the network. In dilute solutions, the ion swelling pressure can be approximated by means of the van t Hoff's law [20] using concentration values c_i^g and c_i^s of i th mobile ions in the gel and in the surrounding solution, respectively (see Equation (A2) in Appendix A). This pressure, when present, leads to an additional water uptake by the hydrogel network. The values of c_i^g depend on the concentration of fixed charges in the gels, which depends in turn on the degree of substitution of ionizable groups, on the pH value, and on the ionic content of the external medium (values of c_i^s).

The osmotic pressure due to the concentration variation of ionized polymer groups and due to the distribution of mobile ions as well as the locally different gel swelling and shrinking were numerically investigated in [26,27] by applying the coupled chemo-electromechanical multi-field formulation for polyelectrolyte gels using the finite element method. The gel swelling behavior was considered in dependence on the acid dissociation constant value K_a for ionizable polymer groups and on the change of the pH value or salt concentration in solution [28,29]. In [30], the influence of a change of ambient conditions was simulated for temperature-sensitive polyelectrolyte hydrogels.

Selectivity and sensor response to various interfering molecules at physiological serum concentrations are two of the key criteria that should be addressed when characterizing the performance of the glucose sensor. In recent years, numerous attempts have been made to develop a miniature, enzyme-free glucose sensor, based on a hydrogel with incorporated phenylboronic acid groups as glucose detecting elements [1–3,25]. Other species that ligand to phenylboronic acid can affect the ionization state of these groups and, consequently, the sensor response. In this regard, it is necessary to investigate the potential interference and its effect on the glucose signal.

In the present study, we examined the dependence of glucose sensing upon interferences by fructose and human serum albumin at physiological pH and physiological levels of interfering molecules. We calculated values of the gel swelling pressure in the presence of glucose and fructose in solution and experimentally evaluated these values by means of microfabricated piezoresistive hydrogel-based sensors. We determined the calibrating and measuring procedures for simultaneous and continuous monitoring of analyte concentrations, pH value, and ionic strength. A calibration algorithm was proposed and verified using a sensor array for several metabolic physiological parameters. The output characteristics of the sensors were measured taking into account the investigated cross-sensitivities of polyelectrolyte hydrogels.

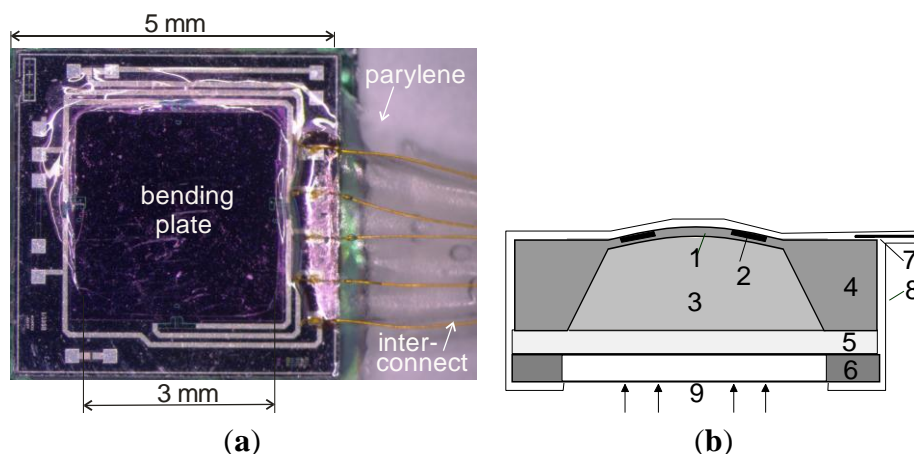
2. Experimental Section

2.1. Sensor Design

Silicon-based microsensors are capable of measuring the swelling pressure from stimuli-responsive hydrogels and, hence, the concentrations of the target analytes as shown in Figure 1. For the design of the chemical sensors, commercially available pressure sensor chips C41/1 (AktivSensor GmbH/Epcos AG, Stahnsdorf, Germany) with a flexible 20 μm thin silicon bending plate and with an integrated piezoresistive Wheatstone bridge at the plate surface were employed as mechano-electrical transducer for the transformation of the plate deflection due to the swelling pressure into an electrical output

signal V_{out} . The calibration procedure for the sensors was performed with the help of a pressure controller and a calibration curves were obtained.

Figure 1. Hydrogel-based biochemical dip sensor: (a) frontside photograph of the sensor and (b) sensor design: 1 bending plate (3 mm × 3 mm × 0.02 mm), 2 mechano-electrical transducer (piezoresistive bridge), 3 swellable hydrogel, 4 Si chip (5 mm × 5 mm × 0.39 mm), 5 porous hydrophilic Anopore™ Al₂O₃ membrane (5 mm × 5 mm × 0.06 mm), 6 substrate, 7 interconnect, 8 hermetic parylene C coating (CVD, $d = 3 \mu\text{m}$), 9 measuring solution.



The polymeric hydrogel was deposited into the cavity at the back side of the silicon chip and closed with a porous biocompatible and hydrophilic Anopore™ Al₂O₃ membrane (Whatman Ltd, thickness 60 μm , pore size 200 nm). This membrane provides a low protein binding for permanent implants [31]. The solution and analyte molecules diffuse into the chip cavity through the membrane, induce the swelling process of the hydrogel, and lead to a change in the silicon plate deflection. The plate deflection due to the swelling pressure change causes a stress state change inside the plate and therefore a change of the resistivity of the piezoresistors affecting proportionally the output voltage V_{out} of the sensors. An increasing value of V_{out} corresponds to hydrogel swelling, whereas decreasing of V_{out} corresponds to deswelling.

The sensors were wire-bonded to a printed circuit board and coated with a 3 μm thick hermetic biocompatible parylene C layer using chemical vapor deposition (CVD) as described in [9] to protect the sensors and electrical connections during wet testing. This layer was removed from the membrane surface on the sensor's back side in order to allow for the diffusion of analytes and solution into the chip cavity. Finally, the sensors were connected to a measuring set-up, which was able to monitor the output signals of the sensors.

As regards the hydrogel loading into the chip cavity, the thickness of the dried hydrogel layer was well adapted for the cavity depth preventing a large underloading which could lead to a dead response zone. The sensors with the dried hydrogel layer in the chip cavity showed a value of the offset voltage smaller than 20 mV (see Figure B1 in Appendix B). After the sensor preparation, an initial gel conditioning procedure was performed: an initial gel swelling in a glucose-free phosphate-buffered saline (PBS, pH 7.4, ionic strength $I = 0.15 \text{ M}$) for 24 h. The value $V_{out,0}$ of the sensor output voltage at steady state of the swollen gel was determined and then used as reference value (see Figure B1 in Appendix B). Only after the accomplished conditioning procedure, the sensor signal was measured in

PBS solutions with different analyte contents. In the PBS solution containing an analyte (e.g., glucose, see Figure B3 in Appendix B), a further gel swelling was observed and the corresponding value V_{out} of the sensor output voltage was measured. The curves in Figure B3 characterize the sensor response to the glucose concentration changes. As the piezoresistive pressure sensor chips showed excellent stable and dynamic properties with a response time $t < 1$ s, the long-term stability of the sensors and their response time were solely determined by the stability of the hydrogel characteristics and by the gel swelling/deswelling kinetics, respectively. The possibilities to improve the response time of the sensors will be considered in Section 3.1.3.

The change of the gel swelling pressure induced by the change of the analyte concentration was estimated using the value $\Delta V_{\text{out}} = V_{\text{out}} - V_{\text{out},0}$ and the calibration curve $\Delta\pi = f(\Delta V_{\text{out}})$ of the sensor (Figure B2 in Appendix B).

2.2. Materials and Methods

The monomers used for the preparation of the gels were obtained as follows: acrylamide (AAM, Fisher Scientific), 3-acrylamidophenylboronic acid (3-AAMPBA, Frontier Scientific, Logan, UT, USA), and *N,N*-methylenebisacrylamide (BIS, Sigma-Aldrich). Hydroxypropylmethacrylate (HPMA), *N,N*-dimethylaminoethyl methacrylate (DMAEMA), and tetra-ethyleneglycol dimethacrylate (TEGDMA) were purchased from Polysciences, Inc. (Warrington, PA, USA). The monomers were used as received. 2-hydroxy-4'-(2-hydroxyethoxy)-2-methyl-propiophenone (HHMP, Sigma-Aldrich), 1-vinyl-2-pyrrolidinone (v-pyrol, Sigma-Aldrich), dimethyl sulfoxide (DMSO, Sigma-Aldrich), 4-(2-hydroxyethyl)piperazine-1-ethanesulfonic acid (HEPES, Sigma-Aldrich), ammonium peroxydisulfate (APS, Sigma-Aldrich), *N,N,N',N'*-tetramethylethylenediamine (TEMED, Sigma-Aldrich), D(+)-glucose (Roth), and Dulbecco's phosphate-buffered saline solution (1X PBS, Sigma-Aldrich) were also used as received.

N-isopropylacrylamide (NIPAAm, ACROS) was purified by recrystallisation from hexane and afterwards dried in vacuum. Diethyl ether, ethyl acetate, dioxane, and tetrahydrofuran (THF) were distilled over potassium hydroxide. Cyclohexanone was purified by distillation over calcium hydride. 2,2'-Azobis(isobutyronitrile) (AIBN) was recrystallized from methanol. All other reagents were of analytical grade. The 2-(dimethylmaleinimido)acrylamide (DMIAAm) monomer was synthesized according to [32]. 1-[3-(chloro-dimethyl-silanyl)-propyl]-3,4-dimethylmaleimide was prepared according to [33].

2.2.1. Glucose-Sensitive AAm/3-AAMPBA/BIS Hydrogels

A cross-linked glucose-sensitive copolymer of acrylamide and 3-acrylamidophenylboronic acid (AAm/3-AAMPBA) containing AAm/3-AAMPBA/BIS at a nominal mole ratio of 80/20/0.25 was prepared by free-radical crosslinking copolymerization as described in [3]. Stock solutions of AAm and BIS were prepared in distilled water. Appropriate amounts of the two stock solutions were mixed in a vial with TEMED. In order to dissolve 3-AAMPBA into the pre-gel solution, 1M NaOH was added into the vial. The free-radical initiator APS was introduced after purging the vial with N_2 gas for 10 min, after which the pre-gel solution was injected into a cavity (thickness 400 μm) between two square plates (polycarbonate and poly(methyl methacrylate)) of surface area 60 cm^2 . The total

monomer concentration in the pre-gel solution was 30.2 wt%. After approximately 16 h of reaction at room temperature, the hydrogel slab was removed from the mold and washed for at least two days with deionized water and PBS buffer (pH 7.4, ionic strength 0.15M) before testing. In sugar-free PBS buffer at physiological pH and ionic strength, the hydrogel contains 58 wt% water. The dried hydrogel foils (thickness $d_0 = 330 \mu\text{m}$) were prepared by evaporation of water at room temperature and then cut into pieces. The pieces of surface area $S_0 = 3 \text{ mm} \times 3 \text{ mm}$ were used for the sensor.

2.2.2. pH-Sensitive HPMA/DMAEMA/TEGDMA Hydrogels

The pH-responsive hydrogel is based on three monomers: hydroxypropyl methacrylate (HPMA), *N,N*-dimethylaminoethyl methacrylate (DMAEMA) and tetra-ethylenglycol dimethacrylate (TEGDMA). The DMAEMA monomer contains a pH-sensitive tertiary amine, HPMA was included to obtain a transition pH close to the physiological range [9] and tetra-ethyleneglycol dimethacrylate (TEGDMA) acts as crosslinker.

A detailed description of the synthesis procedure of the cationic polyelectrolyte hydrogel containing HPMA/DMAEMA/TEGDMA at a nominal mole ratio 70/30/2 is described elsewhere [9,34]. Appropriate amounts of monomers HPMA and DMAEMA, crosslinker TEGDMA as well as accelerator TEMED were mixed in a vial to obtain a pre-gel solution, which was then purged with N_2 gas for about 10 min. Shortly thereafter, the initiator APS was added to the pre-gel solution and the mixture was vortexed for about 5 s before being injected into a cavity (thickness $400 \pm 10 \mu\text{m}$) between two square glass plates of surface area 64 cm^2 . The hydrogel slab was removed from the glass plate after approximately 4 h of reaction then washed with PBS solution for at least 2 days to remove unreacted chemicals prior to testing.

In case of the cationic HPMA/DMAEMA/TEGDMA-hydrogels, the tertiary amine groups of the DMAEMA become ionized for pH values below the base dissociation constant of DMAEMA ($\text{pK}_b = 7.8$). Therefore, a phase transition can be observed by altering the pH towards acidic conditions [35].

2.2.3. PNIPAAm-DMAAm-DMIAAm Terpolymer

The photo cross-linkable PNIPAAm-DMAAm-DMIAAm terpolymer (at a mole ratio 66.3/30.7/3) was obtained by free radical polymerization of *N*-isopropylacrylamide (NIPAAm), dimethylacrylamide (DMAAm) and 2-(dimethylmaleinimido)acrylamide (DMIAAm) initiated with AIBN at $70 \text{ }^\circ\text{C}$ in dioxane with a total monomer concentration of 0.55 mol/L under nitrogen for 7 h. The polymer was precipitated in diethylether and purified by reprecipitation from THF into diethylether (1:3).

The DMIAAm-chromophore was selected for cross-linking because it is known to form stable dimers. The DMIAAm-chromophore reacts via a [2 + 2]-cycloaddition under irradiation. By using thioxanthone as photo sensitizer, a complete conversion of the chromophores could be achieved within a few minutes [33].

The adhesion promoter layer was prepared by absorbing 1-[3-(chloro-dimethyl-silanyl)-propyl]-3,4-dimethylmaleimide from 0.3 vol% solution in dicyclohexyl on the $\text{Si}/\text{Si}_3\text{N}_4$ surface of the chip bending plate for 24 h. The substrates were rinsed with chloroform. Pre-gel solution was deposited into the chip cavity by pipetting of 10 μL cyclohexanone solution containing 10 wt% polymer and 2 wt% (with respect to the polymer) thioxanthone sensitizer. The polymer films were dried at $60 \text{ }^\circ\text{C}$ for 15 min

and then under vacuum at 20 °C for 5 min. The dry films were cross-linked by UV irradiation, using a mercury lamp producing an irradiance at the substrate plane of 1.7 mW/cm².

The PNIPAAm-DMAAm-DMIAAm terpolymer has a higher value of the volume phase transition temperature T_{cr} ($T_{cr} = 43$ °C) than PNIPAAm ($T_{cr} = 33$ °C) due to the additional hydrophilic DMAAm component [10,36]. In the physiological temperature range between 36 °C and 40 °C, the PNIPAAm-DMAAm-DMIAAm hydrogel is in its swollen state.

2.2.4. Solution Characterization

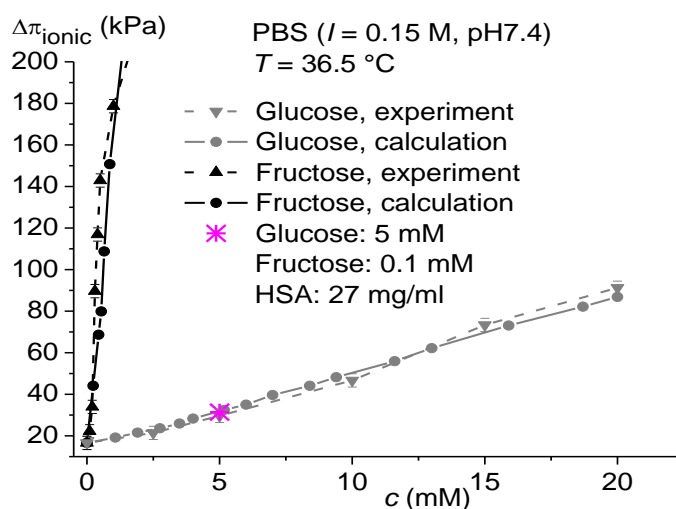
D(+)-glucose (Roth) and d(-)-fructose (Acros Organics) were dissolved in phosphate buffered saline (PBS, pH7.4) solutions of ionic strength $I = 0.15$ M. The pH value of PBS was adjusted with HCl or with NaOH and was measured using a Knick pH meter with pH/Pt-1000 probe.

3. Results and Discussion

3.1. Sensors for Glucose Concentration

The glucose-sensitive hydrogel used in this study in glucose sensors was a copolymer of acrylamide and 3-acrylamidophenylboronic acid (AAm/3-AAmPBA). Figure 2 shows the effect of glucose on the response of one sensor (sensor 1) within a range from 0 mM to 20 mM of glucose. Figure B5a in Appendix B shows the data scatter of the four repeated measurements for the sensor 1, and Figure B5b shows the measuring results for three sensors. The sensors with phenylboronic acid (PBA)-containing gel demonstrated an increasing gel swelling pressure with increasing glucose concentration c_G in PBS solution (pH7.4, $I = 0.15$ M). From the plot of the sensor characteristic, the sensor's sensitivity was estimated to be 3.7 kPa/mM over the range 0–20 mM glucose. The measurement uncertainty was calculated according to [37,38] (see Appendix B). The value of the expanded uncertainty $u_{exp}(\pi_A)$ was estimated to be 3.2 kPa and shown in Figure 2 using error bars.

Figure 2. Response of the sensor 1 with AAm/3-AAmPBA/BIS hydrogel and corresponding calculated values of the gel swelling pressure in dependence on glucose (▼) and fructose (▲) concentration, respectively, in PBS solutions (pH 7.4, ionic strength 0.15 M) at 36.5 °C and in PBS solution with $c_G = 5$ mM, $c_F = 0.1$ mM, and $c_{HSA} = 27$ mg/mL (⊙).



The pendant groups of phenylboronic acid are present in both an uncharged trigonal form and a charged tetrahedral boronate at physiological pH [39–41]. Phenylboronic acid exists in equilibrium between the uncharged and the charged form. The complex formation between the uncharged form and glucose is unstable because of its high susceptibility to hydrolysis, while charged phenylboronic acid groups are able to form a stable complex with glucose [2]. The complex formation between the charged phenylboronic acid groups and glucose causes a shift in the equilibrium towards an increase of charged phenylboronic acid groups. Therefore, the total amount of charged phenylboronic acid groups increases when glucose is added, thereby increasing the osmotic swelling pressure within the gel, which subsequently leads to the gel swelling.

The charged form of PBA is characterized by a pK_a value, which in the absence of glucose is given by $pK_a = 8.86$ [1]. Binding of glucose is characterized by a binding constant of the glucose molecule to PBA, $K_G = 9.1$ mM. In the present work, these values were used to calculate the gel osmotic pressure in the presence of glucose according to Equation (A9) (see Appendix A), which is based on the value of the Donnan ratio λ .

In order to calculate the value of λ , we reformulated Equation (A10) for an anionic gel ($z = -1$) in a uni-univalent electrolyte solution (the valence of ions $z_i = \pm 1$) as:

$$\alpha = \frac{1 + \sum_n c_{\alpha_n} / K_{\alpha_n}}{1 + \lambda \cdot c_{H^+} / K_a + \sum_n c_{\alpha_n} / K_{\alpha_n}} = \frac{1}{1 + \lambda a_1} \quad (1)$$

and Equation (A8) as:

$$\lambda - 1/\lambda = b/(1 + a_1\lambda) \quad (2)$$

using the substitutions:

$$a_1 = \frac{c_{H^+} / K_a}{1 + \sum_n c_{\alpha_n} / K_{\alpha_n}} \quad (3)$$

and:

$$b = c_0^g / c^s \quad (4)$$

Here,

- $c_{H^+} = 10^{-pH}$ is the concentration of hydrogen ions related to the pH of the environment;
- c_0^g , K_a , and α are the concentration, the acid dissociation constant, and the degree of ionization, respectively, of the ionizable polymer groups;
- c_{α_n} and K_{α_n} are the concentration and dissociation constant, respectively, of the n th analyte species;
- c^s is the total ion concentration in the solution (see Equation (A4) in Appendix A).

Further, Equation (2) can be rewritten as third-order polynomial

$$a_1\lambda^3 + \lambda^2 - (a_1 + b)\lambda - 1 = 0 \quad (5)$$

In order to solve Equation (5), we calculated the value of c_0^g using the input data of the dried gel layer, and then the value of b using Equation (4).

The input data of the polymer layer shown in Tables 1 and 2 were used for the calculation of the concentration c_0^g of the ionizable PBA groups. Here, ρ_p and $m_p = \rho_p V_0$ are the density and the mass of the dried gel layer, respectively, M_1 and N_1 denote the molar mass and the number of the acrylamide (AAM, C_3H_5NO) monomer units, respectively, M_2 and N_2 denote the molar mass and the number of the 3-acrylamidophenylboronic acid (3-AAMPBA, $C_9H_{10}BNO_3$) monomer units, respectively, M_3 and N_3 denote the molar mass and the number of N,N' -methylene-bisacrylamide (BIS, $C_7H_{10}N_2O_2$), respectively. Taking into account the polymer composition, we obtained for the mole numbers N_1 , N_2 and N_3 of AAM, 3-AAMPBA and BIS, respectively in the gel sample volume V_0

$$N_1 = m_p \xi_1 / (M_1 \xi_1 + M_2 \xi_2 + M_3 \xi_3) \quad (6)$$

$$N_2 = m_p \xi_2 / (M_1 \xi_1 + M_2 \xi_2 + M_3 \xi_3) \quad (7)$$

$$N_3 = m_p \xi_3 / (M_1 \xi_1 + M_2 \xi_2 + M_3 \xi_3) \quad (8)$$

Here, ξ_1 , ξ_2 and ξ_3 are the mole fractions of AAM, 3-AAMPBA and BIS, respectively. The value $c_0^g = 2.23$ M of the ionizable PBA groups concentration in the pre-swollen gel sample (thickness $d_1 = 400$ μm , volume $V_1 = 3.6$ μL) was calculated as:

$$c_0^g = N_2 / V_1 \quad (9)$$

and used in Equation (4). Solving Equation (5), we obtained an equilibrium value of the Donnan ratio λ ($\lambda > 1$), that was used in Equation (A9) for the calculation of the gel osmotic pressure in the presence of analytes in the solution. The values of a_1 and λ for the different glucose concentrations in PBS solution with pH7.4 and $I = 0.15$ M as well as the corresponding calculated values of the ionic swelling pressure $\Delta\pi_{\text{ionic}}$ at $T = 36.5$ $^\circ\text{C}$ are shown in Table C1 (Appendix C). Figure 2 compares the measured and the calculated values of the gel swelling pressure $\Delta\pi_{\text{ionic}}$ for the AAM/3-AAMPBA/BIS hydrogel layer in PBS solutions (pH7.4, ionic strength 0.15 M) with different sugar concentrations at 36.5 $^\circ\text{C}$.

Table 1. Parameters of the investigated AAM/3-AAMPBA/BIS layer.

| d_0 , μm | S_0 , mm^2 | V_0 , L | ρ_p , g/cm^3 | m_p , g |
|--------------------------|--------------------------|-----------------------|-------------------------------|-----------------------|
| 330 | 9 | 3×10^{-6} | 1.29 [42] | 3.8×10^{-3} |

Table 2. Composition of the investigated AAM/3-AAMPBA/BIS layer.

| Monomer | M , g/mol | N , mol | ξ , $\text{mol}\%$ |
|-------------------------------|-------------------------|-----------------------|---------------------------|
| AAM (C_3H_5NO) | 71.08 | 3.2×10^{-5} | 80 |
| 3-AAMPBA ($C_9H_{10}BNO_3$) | 190.99 | 8×10^{-6} | 20 |
| BIS ($C_7H_{10}N_2O_2$) | 154.17 | 1×10^{-7} | 0.25 |

Our microfabricated sensors demonstrated a sufficient sensitivity of 3.7 kPa/mM over the range 0–20 mm glucose in PBS solutions with physiological pH and ionic strength values. For comparison,

Table 3 shows the results for microfabricated implantable glucose sensors from other works. In [1], the sensitivity of a capacitive glucose sensor with an acrylamide/methacrylamidophenylboronic acid/*N,N*-methylenebisacrylamide (AAm/MAAmPBA/BIS) hydrogel confined in the $2.8 \times 2.8 \times 0.2 \text{ mm}^3$ cavity was achieved to be 0.15 kPa/mM over the glucose concentration range 0–20 mM in the linear region of the sensor characteristic. In [43], the piezoresistive glucose sensor with an acrylamide/3-acrylamidophenylboronic acid/*N*-3-dimethyl-aminopropyl acrylamide/*N,N*-methylenebisacrylamide (AAm/3-AAmPBA/DMAPAAm/BIS) hydrogel in the chip cavity of $1 \times 1 \times 0.4 \text{ mm}^3$ displayed a sensitivity of 0.005 kPa/mM over the range 0–20 mM glucose.

Table 3. Parameters of microfabricated implantable glucose sensors.

| Transducer | Hydrogel | Sensitivity, kPa/mM | Dimensions of Cavity with Gel, mm^3 | References |
|----------------|--------------------------|---------------------|--|--------------|
| piezoresistive | AAm/3-AAmPBA/BIS | 3.7 | $3 \times 3 \times 0.37$ | present work |
| capacitive | AAm/MAAmPBA/BIS | 0.15 | $2.8 \times 2.8 \times 0.2$ | [1,2] |
| piezoresistive | AAm/3-AAmPBA/DMAPAAm/BIS | 0.005 | $1 \times 1 \times 0.4$ | [43] |

3.1.1. Cross-Sensitivity to Interferents

An apparent problem with this glucose sensing mechanism is that PBA cannot distinguish glucose from other cis-diol molecules and may give rise to errors when the glucose measurements are carried out in presence of other sugar molecules, for instance, fructose, which is also found in blood. Although the normal physiological level of fructose is approximately 500 times smaller than that of glucose (8 μM vs. 5.5 mM, respectively), the binding affinity of PBA for fructose exceeds that for glucose by a factor of 40 [2–4]. Binding of fructose is characterized by a binding constant of the fructose molecule to PBA, $K_F = 0.23 \text{ mM}$ [1]. In the present work, this value of K_F was used to calculate the gel swelling pressure $\Delta\pi_{\text{ionic}}$ in PBS solutions containing fructose according to Equations (3)–(5), and (A9) (Figure 2). The values of a_1 and λ for the different fructose concentrations in PBS solution with pH7.4 and $I = 0.15 \text{ M}$ as well as the corresponding calculated values of the ionic swelling pressure $\Delta\pi_{\text{ionic}}$ at $T = 36.5 \text{ }^\circ\text{C}$ are shown in Table C2 (Appendix C).

In order to investigate the potential interference, the sensor signal was measured in PBS solutions containing fructose within a range from 0 mM to 2.5 mM. Figure 2 shows a greater sensor response to fructose than to glucose. However, at small fructose concentrations $c_F < 0.1 \text{ mM}$ no influence of fructose on the sensor signal was observed. As a step to progressively move towards *in vivo* experiments, an additional test was performed in PBS solution containing 5 mM glucose, 0.1 mM fructose and 27 mg/mL human serum albumin (HSA) in order to mimic body fluids (Figure 2). No changes were observed in the gel swelling degree due to adding the protein within the physiological concentration range.

The response of PBA-containing hydrogels to various mono- and disaccharides as well as to lactate and glycerol has been tested in [1,17,39,44] taking into account the binding affinities at physiological pH and physiological levels of interfering molecules. A complete analysis of chemical interference with sensor function would also include the effects of polysaccharides and glycoproteins as well as the effects of such essential anti-inflammatory medicines as acetylsalicylic acid (aspirin), iso-butyl-propanoic-phenolic acid (ibuprofen) and *N*-acetyl-*p*-aminophenol (paracetamol, acetaminophen).

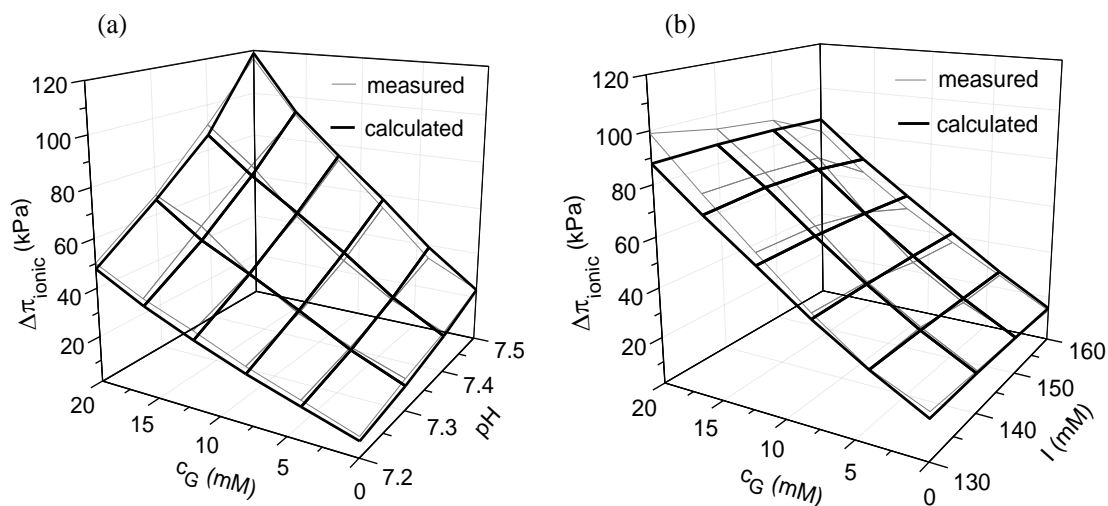
Potential interferences could cause a glucose measurement error. The concentration fluctuations of the interfering species will add a noise to the device response which has to be investigated comprehensively in our future studies.

It should be noted, that the use of hydrogels, which are more specific to glucose molecules provides an additional possibility to minimize the interference by other species that may be present in the physiological environment. The glucose selectivity of PBA can be improved via incorporation of quaternary amines into the hydrogel as discussed in [2,4]. Efforts to improve the sensor performance for practical use by applying a copolymer acrylamide/3-acrylamidophenylboronic acid/*N*-(3-dimethylaminopropyl acrylamide) (AAm/3-AAmPBA/DMAPAAm) are currently underway in our institute.

3.1.2. Effects of pH and Ionic Strength Changes

In order to investigate the influence of the environmental pH change on the calibration curves of the glucose sensors, the sensor signal was monitored in glucose-containing PBS solutions with different pH values. Figure 3a shows the response of the sensor 1 with AAm/3-AAmPBA/BIS hydrogel plotted over the glucose concentration and pH of the PBS solution (ionic strength $I = 0.15$ M). The fixed charge density on the AAm/3-AAmPBA/BIS polymer backbone increases with increasing pH value due to the ionization of the anionic PBA groups, thereby increasing the osmotic swelling pressure within the gel, which subsequently leads to the gel swelling.

Figure 3. Ionic component $\Delta\pi_{\text{ionic}}$ of the gel swelling pressure measured by means of the sensor 1 with AAm/3-AAmPBA/BIS hydrogel at 36.5 °C in PBS solutions (ionic strength $I = 0.15$ M) plotted over the glucose concentration c_G and pH (a) and in PBS solutions (pH7.4) plotted over the glucose concentration c_G and ionic strength I (b) as well as corresponding calculated values of $\Delta\pi_{\text{ionic}}$. The values of a_1 , b , and λ used for the calculation are shown in Tables C3 and C4 (Appendix C).



An increase of the ionic strength of a solution has an opposite effect on the response of the glucose sensor (Figure 3b). The sensor signal was measured in glucose-containing PBS solutions (pH7.4) with different values of the ionic strength. Figure 3b shows a decrease of the gel swelling pressure with

increasing value of the ionic strength. An increase of the environmental ionic strength enhances the osmotic pressure outside the hydrogel, which pushes the hydrogel to shrink.

From these experiments, it is clear that the correct value of the glucose concentration in solution can be determined only in the case of known pH- and I -values because the swelling of a glucose-sensitive hydrogel results from the interplay of the glucose concentration, pH and the ionic strength of the solution. The cross-sensitivity of a polyelectrolyte glucose-sensitive gel can be eliminated by using two reference sensors for simultaneous pH and ionic strength measurements. The corrected values of the glucose concentration could be estimated with the help of the calibration curves of these three sensors (see Section 3.4).

3.1.3. Response Time

The gel response time depends on the cooperative diffusion coefficient and on the square of the sample dimension. Scaling to micro-dimensions enhances the time response. Consequently, a reduction of the sample size improves the sensor performance. However, a reduction of the gel thickness is limited by the necessity to obtain a sufficiently high sensor signal and, consequently, a sufficient sensitivity. It is feasible to achieve an optimum between the sensor signal amplitude and the sensor response time by using:

- (1) porous gels. A response time reduction of about 80% was observed compared to sensors with non-porous hydrogels [45]. However, the porous structure affects the mechanical stability of the gel and, consequently, the long-term stability of the sensor sensitivity, which needs to be improved.
- (2) composite as well as hybrid materials. A significant reduction (of 72%, compared to the homogeneous hydrogel) of the sensor response time was achieved for the hybrid hydrogel with incorporated hygroscopic fibers which accelerated the diffusion of the solution in the gel and, consequently, the gel swelling/deswelling [19]. The incorporated hydrophilic porous fibres led to a faster, and at the same time, increased solution uptake.
- (3) the method of initial rate determination of the solution uptake. It was found that the value v of this rate depends on the initial concentration gradient ($c_{\alpha}^0 - c_{\alpha 0}$) of the analyte between the solution and the gel [10]. With the help of the values v_1 and v_2 for two solutions with a known concentration $c_{\alpha,1}^0$ and with an unknown one $c_{\alpha,2}^0$, the value of $c_{\alpha,2}^0$ can be estimated (see Equation (B1) in Appendix B). By applying this method, the measuring time t_m which is necessary to determine the glucose concentration in PBS solution was essentially shortened from the time to reach a full saturation of the solution uptake to the time which is necessary for the initial rate determination ($t_m \leq 3$ min, see Figure (B4) in Appendix B).

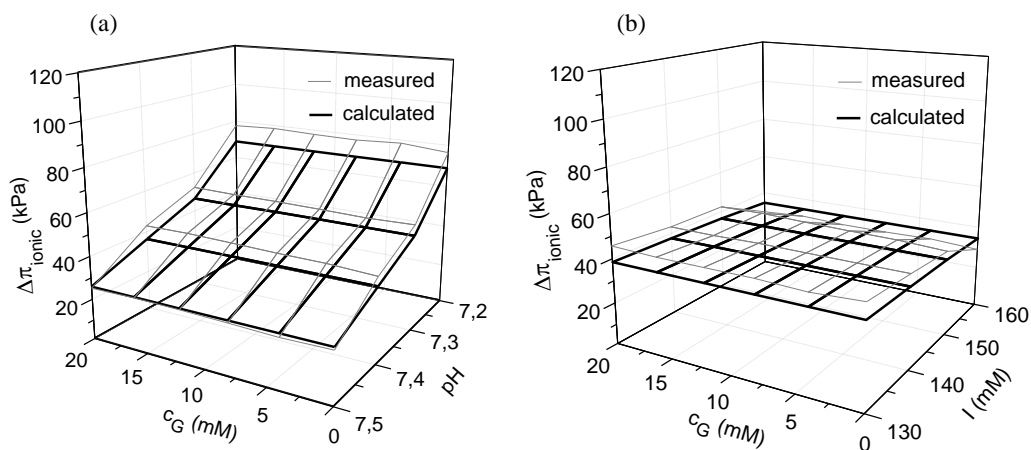
3.2. pH Sensors

The pH-responsive HPMA/DMAEMA/TEGDMA hydrogel was used in pH sensors. The DMAEMA monomer contains pH-sensitive tertiary amines, HPMA was included to obtain a transition pH close to the physiological range near pH 7.4. The sensing mechanism is based on the protonation of the tertiary amines on the DMAEMA backbone. At pH values lower than pH 8, elevated backbone protonation

temporarily increases the osmotic swelling pressure within the hydrogel (Figure 4a). From the plot of the sensor characteristic, the sensor’s sensitivity was estimated to be 17.4 kPa per 0.1 pH over the pH range 7.2–7.5 at $I = 0.15$ M. Similar as in Section 3.1, dried gel pieces of the same size (3 mm × 3 mm × 0.33 mm) were used for pH sensors.

In order to verify the insensitivity of HPMA/DMAEMA/TEGDMA gel to glucose, the sensor signal was measured in PBS solutions containing glucose within a range from 0 mm to 20 mm (Figure 4). No changes were observed in the gel swelling degree due to adding of glucose. This confirms the reasonability of the use of HPMA/DMAEMA/TEGDMA gel in a reference sensor for pH measurements.

Figure 4. Ionic component $\Delta\pi_{\text{ionic}}$ of the gel swelling pressure measured by means of the sensor with HPMA/DMAEMA/TEGDMA hydrogel at 36.5 °C in PBS solutions (ionic strength $I = 0.15$ M) plotted over the glucose concentration c_G and pH (a) and in PBS solutions (pH7.4) plotted over the glucose concentration c_G and ionic strength I (b) as well as corresponding calculated values of $\Delta\pi_{\text{ionic}}$.



In the case of the cationic HPMA/DMAEMA/TEGDMA-hydrogels, the tertiary amine groups of the DMAEMA become ionized for pH values below a base dissociation constant of DMAEMA ($pK_b = 7.8$). In this study, we estimated the value of the fraction α of the ionized cationic polymer groups which only bind protons as:

$$\alpha = \frac{1}{1 + \lambda^{-1} \cdot c_{OH^-} / K_b} = \frac{1}{1 + \lambda^{-1} a_2} \tag{10}$$

using the substitution:

$$a_2 = c_{OH^-} / K_b \tag{11}$$

Here, $c_{OH^-} = 10^{-(14-pH)}$ is the concentration of hydroxide ions related to the pH of the environment and K_b denotes the base dissociation constant of the ionizable polymer groups.

In order to calculate the value of λ , we reformulated Equation (A8) for a cationic gel ($z = +1$) in a uni-univalent electrolyte solution (the valence of ions $z_i = \pm 1$) as:

$$\lambda - 1/\lambda = -b/(1 + a_2 \lambda^{-1}) \tag{12}$$

using the substitution from Equation (4).

Further, Equation (12) can be rewritten as third-order polynomial:

$$\lambda^3 + (a_2 + b)\lambda^2 - \lambda - a_2 = 0 \quad (13)$$

In order to solve Equation (13), we calculated the value of c_0^g using the input data of the dried HPMA/DMAEMA/TEGDMA gel layer, and then the value of b using Equation (4).

The input data of the polymer layer shown in Tables 1 and 4 were used for the calculation of the concentration c_0^g of the ionizable DMAEMA groups. Similar, as in Section 3.1, the numbers of monomer units shown in Table 4 were calculated for a dried gel piece of the same size (3 mm × 3 mm × 0.33 mm). The value $c_0^g = 2.06$ M of the ionizable DMAEMA groups concentration in the pre-swollen gel sample (thickness $d_1 = 400$ μm, volume $V_1 = 3.6$ μL) was calculated as:

$$c_0^g = N_{\text{DMAEMA}} / V_1 \quad (14)$$

and used in Equation (4). Solving Equation (13), we obtained an equilibrium value of the Donnan ratio λ ($0 < \lambda < 1$), that was used in Equation (A9) for the calculation of the ionic osmotic pressure of the gel. The values of a_2 , b , and λ for the different pH values of PBS solutions and for the different values of the ionic strength I are shown in Table D1 (Appendix D). Figure 4 compares the measured and the calculated values of the gel swelling pressure $\Delta\pi_{\text{ionic}}$ for the HPMA/DMAEMA/TEGDMA hydrogel layer in PBS solutions at 36.5 °C.

Table 4. Composition of the investigated HPMA/DMAEMA/TEGDMA layer.

| Monomer | M , g/mol | N , mol | ξ , mol% |
|--|----------------|----------------------|-----------------|
| HPMA (C ₇ H ₁₂ O ₃) | 144.17 | 1.7×10^{-5} | 70 |
| DMAEMA (C ₈ H ₁₅ O ₂ N) | 157.20 | 7.4×10^{-6} | 30 |
| TEGDMA (C ₁₆ H ₂₆ O ₇) | 330.37 | 4.9×10^{-7} | 2 |

Our microfabricated pH sensors demonstrated a sufficient sensitivity of 17.4 kPa/0.1pH over the pH range 7.2–7.5 in PBS solutions with the physiological ionic strength of 0.15 M. For comparison, the parameters achieved for microfabricated implantable pH sensors are listed in Table 5. In [25], the sensitivity of a capacitive pH sensor with a methacrylic acid/acrylamide/ethyleneglycol dimethacrylate (MAA/AAm/EGDMA) hydrogel confined in the $2.8 \times 2.8 \times 0.2$ mm³ cavity was 0.15 kPa/0.1pH over the pH range 7.2–7.4.

Table 5. Parameters of microfabricated implantable pH sensors.

| Transducer | Hydrogel | Sensitivity, kPa/0.1pH | Dimensions of cavity with gel, mm ³ | References |
|----------------|--------------------|---------------------------|---|--------------|
| piezoresistive | HPMA/DMAEMA/TEGDMA | 17.4 | $3 \times 3 \times 0.37$ | present work |
| capacitive | MAA/AAm/EGDMA | 0.23 | $2.8 \times 2.8 \times 0.2$ | [25] |

The swelling of a pH-sensitive hydrogel results from the interplay of the pH and the ionic strength of the solution. Figure 4b shows the output characteristics of the pH-sensor in glucose-containing buffered solutions of several series with different ionic strengths. From the plot of the curve at pH7.4, the cross-sensitivity was estimated to be 0.16 kPa/mM over the I -range 130–150 mM. In [9], a pH-sensitive

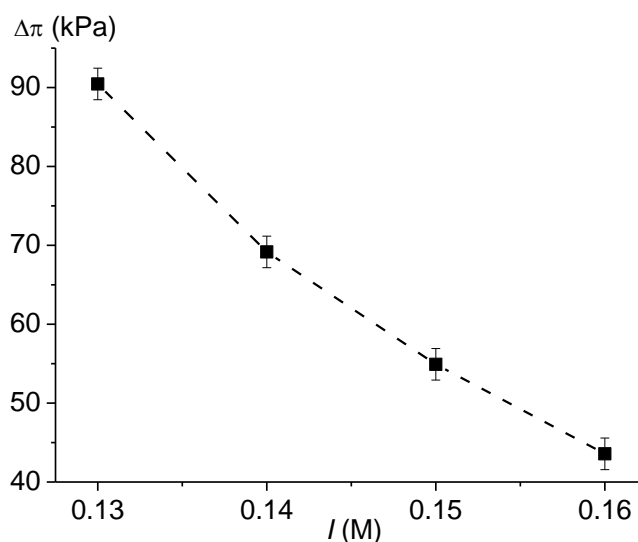
HPMA/DMAEMA/TEGDMA gel confined in a $1.5 \times 1.5 \times 0.4 \text{ mm}^3$ cavity of a piezoresistive sensor displayed a cross-sensitivity of 0.12 kPa/mM to the ionic strength over the I -range 125–150 mM.

The cross-sensitivity of a polyelectrolyte gel can be eliminated by using a reference sensor with a neutral gel for the simultaneous ionic strength measurement. The corrected pH values of the solution could be estimated with the help of the calibration curves of these two sensors.

3.3. Sensors for Ionic Strength

The response of the sensor based on PNIPAAm-DMAAm-DMIAAm hydrogel was measured in PBS solutions with different ionic strengths. Figure 5 shows the output characteristics of the sensor for ionic strength. The hydrogel demonstrates a decrease of the swelling pressure with increasing value of the ionic strength. An increase of the environmental ionic strength enhances the osmotic pressure outside the hydrogel, which pushes the hydrogel to shrink.

Figure 5. Gel swelling pressure $\Delta\pi$ measured by means of the sensor with PNIPAAm-DMAAm-DMIAAm hydrogel at 36.5 °C in dependence on ionic strength I of PBS solution.



3.4. Simultaneous Monitoring of Analyte Concentration, pH Value and Ionic Strength

The hydrogel-based sensors were integrated in a sensor array for the simultaneous monitoring of ionic strength, pH value and glucose concentration in solution. The output signals V_1 , V_2 , and V_3 of the sensor for ionic strength I with the PNIPAAm-DMAAm-DMIAAm hydrogel, of the pH sensor with the HPMA/DMAEMA/TEGDMA hydrogel, and of the glucose sensor with the AAm/3-AAmPBA/BIS gel, respectively, were measured using a set-up, which was able to monitor the output signals from multiple sensor arrays simultaneously. Additionally, the temperature T was controlled with a temperature sensor. With the help of the database containing the calibration curves of the hydrogel-based sensors at different values of pH and ionic strength, the corrected values of pH and glucose concentration were determined using a calibration algorithm developed and verified in this work (Figure E1 in Appendix E).

The data-flow-programme consists of three main parts. In the first module, the output signal V_1 of the PNIPAAm-DMAAm-DMIAAm hydrogel-based sensor and the value T of the temperature are used in order to determine the I -value of the measuring solution with the help of the calibration curves of the sensor for ionic strength. In the second module, the determined I -value and the measured V_2 - and T -values are analyzed using the database of the pH sensor, and the correct pH-value is chosen. In the third module, the determined I - and pH-values as well as the measured V_3 - and T -values are compared with the database of the glucose sensor. As a result, the corrected value of the glucose concentration c_G is estimated.

4. Conclusions

Values of the gel osmotic pressure were calculated in the presence of analytes in the solution and compared with those obtained experimentally by means of hydrogel-based sensors. Layers of analyte-specific hydrogels were incorporated in piezoresistive chemical microsensors. A copolymer with glucose-sensitive phenylboronic acid groups was used in the sensors for glucose concentration. A pH-sensitive, but not responsive to glucose hydrogel containing pH-sensitive tertiary amine groups had served as a functional layer in the pH sensors. In the sensors for ionic strength, a neutral terpolymer was used. The calibrating and measuring procedures for simultaneous and continuous monitoring of analyte concentrations, pH value and ionic strength were determined. A calibration algorithm was developed and verified using a sensor array for several metabolic physiological parameters. The output characteristics of the sensors were measured taking into account the investigated cross-sensitivities of polyelectrolyte hydrogels. With the help of the database containing the calibration curves of glucose sensor at different values of pH and ionic strength, the corrected value of glucose concentration was determined and cross-sensitivities were eliminated.

Acknowledgments

F. Solzbacher, P. Tathireddy, and J. J. Magda are acknowledged for the help with the parylene C coating as well as for the preparation of pre-gel solutions. The authors gratefully acknowledge support of this work from the Deutsche Forschungsgemeinschaft (SPP 1259, grant Ge 779/14-3).

Conflicts of Interest

The authors declare no conflict of interest.

Appendix A. Ionic Osmotic Pressure of Polyelectrolyte Hydrogels

The hydrogel swelling pressure $\Delta\pi$ can be described by the sum of three components $\Delta\pi_{\text{mixing}}$, $\Delta\pi_{\text{elastic}}$, and $\Delta\pi_{\text{ionic}}$ [20–24]:

$$\Delta\pi = \Delta\pi_{\text{mixing}} + \Delta\pi_{\text{elastic}} + \Delta\pi_{\text{ionic}} \quad (\text{A1})$$

In dilute solutions, the ionic component $\Delta\pi_{\text{ionic}}$ of the swelling pressure can be approximated by means of the van t Hoff's law as [20]

$$\Delta\pi_{ionic} = RT \sum_i (c_i^g - c_i^s) \tag{A2}$$

where c_i^g and c_i^s are concentrations of i th mobile ions in the gel and in the surrounding solution, respectively, R the universal gas constant, and T the absolute temperature. The equilibrium state is characterized by the Donnan ratio λ , which describes the distribution of mobile ions between the gel and the solution. In the case of a uni-univalent electrolyte solution (the valence of ions $z_i = \pm 1$) [23]:

$$\lambda = \frac{c_{cations}^g}{c_{cations}^s} = \frac{c_{anions}^s}{c_{anions}^g} \tag{A3}$$

Here, $c_{cations}^g$, c_{anions}^g , $c_{cations}^s$ and c_{anions}^s are the concentrations of monovalent mobile cations and anions in the gel and in the solution, respectively. For the polyelectrolyte gel with anionic side groups, $\lambda > 1$.

The total ion concentration c^s in the solution is given as:

$$c^s = c_{cations}^s + c_{anions}^s \tag{A4}$$

For a uni-univalent electrolyte solution,

$$c_{cations}^s = c_{anions}^s = c^s \tag{A5}$$

and c^s is equal to the ionic strength $I = \frac{1}{2} \sum_i z_i^2 c_i^s$.

At equilibrium, charge neutrality is maintained inside the gel:

$$c_{cations}^g - c_{anions}^g + z\alpha \cdot c_0^g = 0 \tag{A6}$$

with:

$$c_{cations}^g = \lambda \cdot c^s, \quad c_{anions}^g = c^s / \lambda \tag{A7}$$

Here, c_0^g is the concentration of the ionizable groups on the polymer backbone and α is the fraction of ionized polymer groups with the valence z .

Using Equations (A6) and (A7), one obtains [25]

$$\sum_i \lambda^{z_i} z_i c^s + z\alpha \cdot c_0^g = 0 \tag{A8}$$

and the ionic osmotic pressure (using Equation (A2))

$$\Delta\pi_{ionic} = RT \sum_i (\lambda^{z_i} - 1) \cdot c^s \tag{A9}$$

In the case of the polyelectrolyte gel with anionic side groups, the fraction α of polymer groups that are ionized in the presence of analytes in the solution depends on their concentrations and on the pH value of the solution [25]:

$$\alpha = \frac{1 + \sum_n c_{\alpha_n} / K_{\alpha_n}}{1 + \lambda \cdot c_{H^+} / K_a + \sum_n c_{\alpha_n} / K_{\alpha_n}} \tag{A10}$$

Here, $c_{H^+} = 10^{-pH}$ is the concentration of hydrogen ions related to the pH of the environment, K_a the acid dissociation constant of the ionizable polymer groups, c_{α_n} and K_{α_n} the concentration and dissociation constant, respectively, of the n th analyte species.

Appendix B. Piezoresistive Chemomechanical Sensors

After the sensor preparation, an initial gel conditioning procedure was performed: an initial gel swelling in a glucose-free phosphate-buffered saline (PBS, pH7.4, ionic strength $I = 0.15$ M) for 24 h (Figure B1). Only after the accomplished conditioning procedure, the sensor signal was measured in PBS solutions with different glucose contents (Figure B3). The curves in Figure B3 characterize the sensor response to the glucose concentration changes.

Figure B1. Sensor output voltage V_{out} during the gel swelling in PBS buffer (pH7.4, ionic strength 0.15 M) when started from a dried state (an initial gel conditioning procedure).

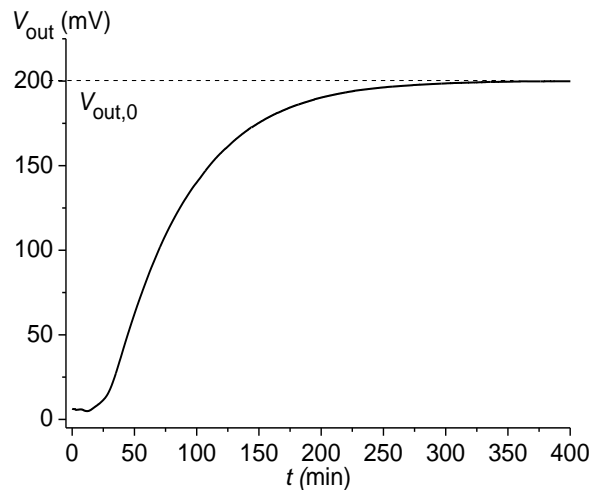


Figure B2. Calibration curve $\Delta\pi = f(\Delta V_{out})$ of the piezoresistive chemomechanical sensors.

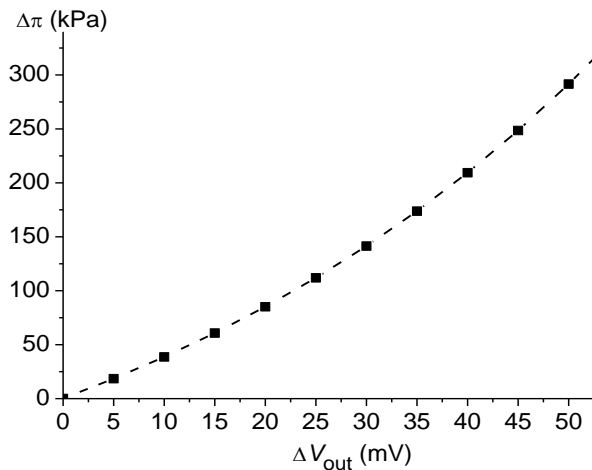
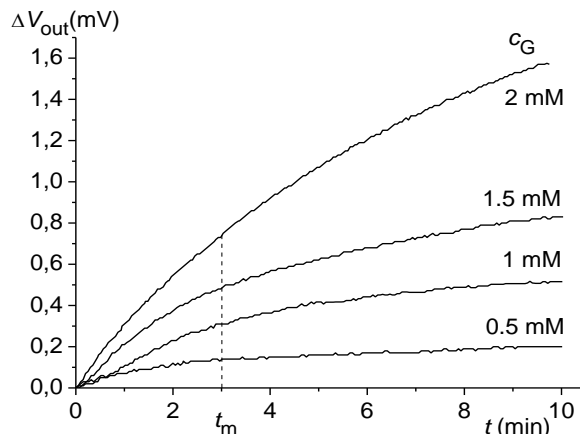


Figure B3. Time-dependent sensor response for different glucose concentration c_G steps in PBS solutions (pH7.4, ionic strength 0.15 M) initially starting from $c_G = 0$ mM.



Method of Initial Rate Determination

In order to shorten the sensor response time, the dependence of the rate v of the initial solution sorption on the initial concentration gradient ($c_{\alpha}^0 - c_{\alpha 0}$) of the analyte between the solution and the gel was used. With the help of the values v_1 and v_2 (see Figure B4) for two solutions with a known concentration $c_{\alpha,1}^0$ and with an unknown one $c_{\alpha,2}^0$, the value of $c_{\alpha,2}^0$ was estimated using Equation (B1).

$$(c_{\alpha,2}^0 - c_{\alpha 0,2}) = (c_{\alpha,1}^0 - c_{\alpha 0,1})(v_2 / v_1) \tag{B1}$$

Figure B4 shows the initial increase in the output voltage for two step values of the gradual glucose concentration change. The values v_1 and v_2 of the initial rate were determined at the time $0 < t_m < 3$ min.

Figure B4. Time-dependent sensor response for two glucose concentration c_G steps from $c_{G0,1}$ to $c_{G,1}^0$ and from $c_{G0,2}$ to $c_{G,2}^0$.

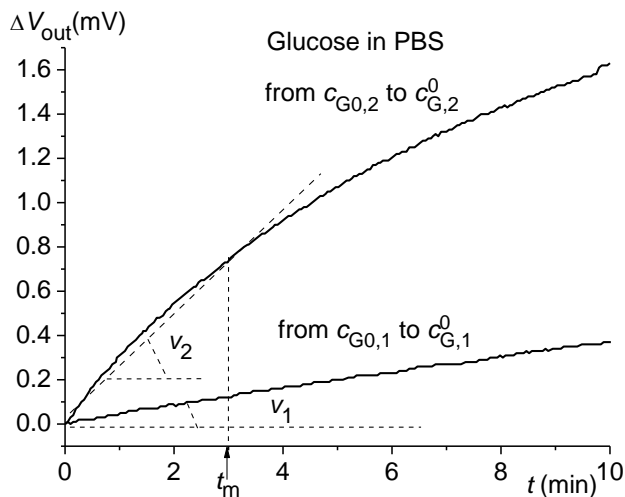
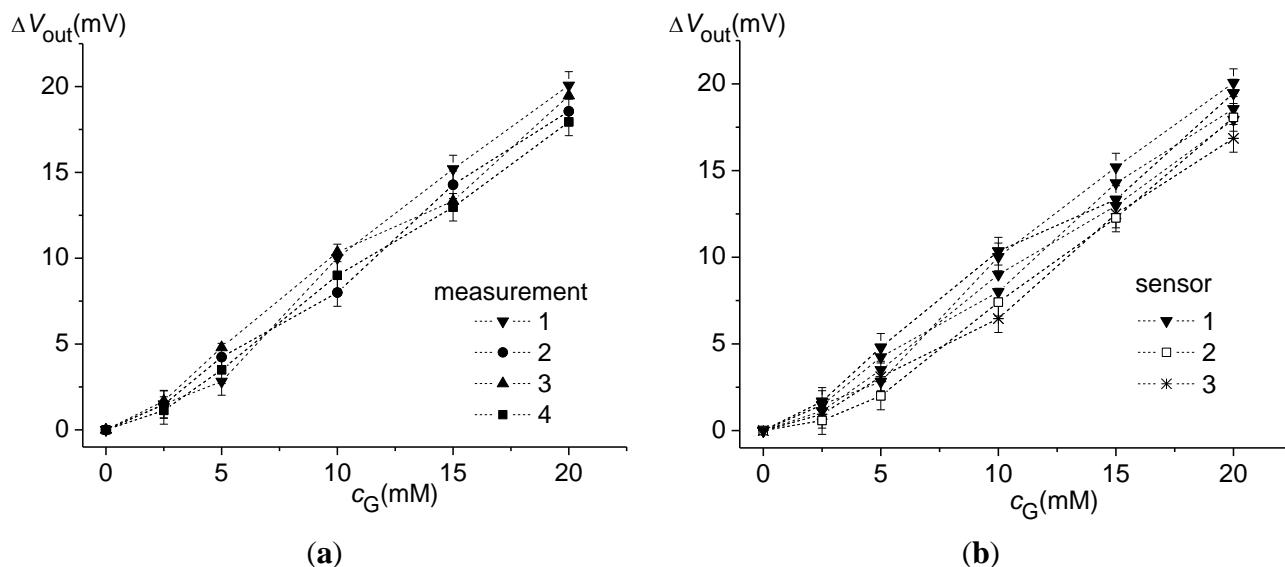


Figure B5. Output characteristics of the glucose sensors with AAm/3-AAmPBA/BIS hydrogel in PBS solutions (pH7.4, ionic strength 0.15 M) at 36.5 °C: (a) results of the four repeated measurements for the sensor 1 and (b) results for three sensors.



Uncertainty of Measurements

The measurement uncertainty was calculated according to the ISO “Guide to the Expression of Uncertainty in Measurement” (GUM) [37]. According to [38], the sensor output voltage V_{out} can be described as a function of the individual voltage components, which are influenced by the target quantity, the disturbing quantities and the internal noise. In the case of glucose sensors, we estimated the combined uncertainty of the analyte-induced voltage $u(V_A)$ as

$$u(V_A) = \sqrt{u(V_T)^2 + u(V_I)^2 + u(V_{pH})^2 + u(V_{int})^2} \tag{B2}$$

taking into account the cross-sensitivities of the glucose sensors with regard to temperature T , ionic strength I , and pH. Here, $u(V_T)$, $u(V_I)$, $u(V_{pH})$, and $u(V_{int})$ are the standard uncertainties due to the disturbing quantities and the internal noise, respectively. The values $u(V_T) = 0.1$ mV, $u(V_I) = 0.5$ mV, $u(V_{pH}) = 0.6$ mV, and $u(V_{int}) = 0.1$ mV were obtained from repeated measurements and were used for the calculation of the combined uncertainty $u(V_A)$ according to Equation (B2). The expanded uncertainty $u_{exp}(V_A)$ was determined using the obtained value $u(V_A) = 0.8$ mV and a coverage factor $k = 2$ as

$$u_{exp}(V_A) = k \cdot u(V_A) \tag{B3}$$

The value of the expanded uncertainty $u_{exp}(\pi_A)$ was estimated to be 3.2 kPa using the value $u_{exp}(V_A) = 1.6$ mV and the calibration curve of the piezoresistive chemomechanical sensors.

Appendix C: AAm/3-AAmPBA/BIS Hydrogel

Table C1. Values of a_1 and λ for the different glucose concentrations c_G in PBS solution with pH7.4 and $I = 0.15$ M as well as the corresponding calculated values of the ionic swelling pressure $\Delta\pi_{\text{ionic}}$ of the investigated AAm/3-AAmPBA/BIS layer at $T = 36.5$ °C. The values $c_0^s = 2.23$ M, $c^s = 0.15$ M, $b = 14.85$, $\text{pK}_a = 8.86$, and $K_G = 9.1$ mM were used for the calculation of $\Delta\pi_{\text{ionic}}$ according to Equations (3)–(5) and (A9).

| c_G, mM | a_1 | λ | $\Delta\pi_{\text{ionic}}, \text{kPa}$ |
|------------------|-------|-----------|--|
| 0 | 28.84 | 1.23 | 16.60 |
| 1 | 25.98 | 1.25 | 19.16 |
| 2 | 23.64 | 1.27 | 22.60 |
| 2.5 | 22.62 | 1.28 | 23.64 |
| 3 | 21.69 | 1.29 | 25.16 |
| 4 | 20.03 | 1.31 | 28.32 |
| 5 | 18.61 | 1.33 | 31.77 |
| 6 | 17.38 | 1.36 | 36.08 |
| 7 | 16.30 | 1.38 | 39.66 |
| 8 | 15.35 | 1.40 | 43.36 |
| 9 | 14.50 | 1.41 | 46.60 |
| 10 | 13.74 | 1.43 | 49.71 |
| 11 | 13.06 | 1.45 | 53.10 |
| 12 | 12.44 | 1.46 | 56.56 |
| 13 | 11.88 | 1.49 | 62.20 |
| 14 | 11.36 | 1.51 | 66.49 |
| 15 | 10.89 | 1.53 | 69.76 |
| 16 | 10.46 | 1.54 | 73.09 |
| 17 | 10.06 | 1.55 | 76.01 |
| 18 | 9.68 | 1.57 | 79.42 |
| 19 | 9.34 | 1.58 | 82.18 |
| 20 | 9.02 | 1.60 | 86.85 |

Table C2. Values of a_1 and λ for the different fructose concentrations c_F in PBS solution with pH7.4 and $I = 0.15$ M as well as the corresponding calculated values of the ionic swelling pressure $\Delta\pi_{\text{ionic}}$ of the investigated AAm/3-AAmPBA/BIS layer at $T = 36.5$ °C. The values $c_0^s = 2.23$ M, $c^s = 0.15$ M, $b = 14.85$, $\text{pK}_a = 8.86$, and $K_F = 0.23$ mM were used for the calculation of $\Delta\pi_{\text{ionic}}$ according to Equations (3)–(5) and (A9).

| c_F, mM | a_1 | λ | $\Delta\pi_{\text{ionic}}, \text{kPa}$ |
|------------------|-------|-----------|--|
| 0 | 28.84 | 1.23 | 16.60 |
| 0.1 | 20.10 | 1.31 | 28.32 |
| 0.2 | 15.43 | 1.38 | 40.39 |
| 0.3 | 12.52 | 1.47 | 58.00 |
| 0.4 | 10.53 | 1.53 | 70.87 |
| 0.5 | 9.09 | 1.60 | 86.85 |
| 0.6 | 7.99 | 1.66 | 101.29 |
| 0.7 | 7.13 | 1.72 | 116.34 |
| 0.8 | 6.44 | 1.77 | 129.30 |
| 0.9 | 5.87 | 1.85 | 150.75 |
| 1.0 | 5.39 | 1.89 | 161.77 |
| 1.3 | 4.34 | 2.04 | 204.66 |
| 2.5 | 2.43 | 2.57 | 370.21 |

Table C3. Values of a_1 and λ for the different glucose concentrations c_G in PBS solutions with $I = 0.15$ M and with the different pH values for the investigated AAm/3-AAmPBA/BIS layer ($c_0^g = 2.23$ M, $b = 14.85$).

| c_G , mM | pH7.2 | | pH7.3 | | pH7.4 | | pH7.5 | |
|------------|-------|-----------|-------|-----------|-------|-----------|-------|-----------|
| | a_1 | λ | a_1 | λ | a_1 | λ | a_1 | λ |
| 0 | 45.71 | 1.15 | 36.31 | 1.19 | 28.84 | 1.23 | 22.91 | 1.28 |
| 1 | 41.18 | 1.17 | 32.71 | 1.20 | 25.98 | 1.25 | 20.64 | 1.30 |
| 2.5 | 35.86 | 1.19 | 28.48 | 1.23 | 22.62 | 1.28 | 17.97 | 1.34 |
| 5 | 29.50 | 1.22 | 23.43 | 1.28 | 18.61 | 1.33 | 14.79 | 1.40 |
| 10 | 21.78 | 1.29 | 17.30 | 1.36 | 13.74 | 1.43 | 10.91 | 1.51 |
| 15 | 17.26 | 1.36 | 13.71 | 1.42 | 10.89 | 1.53 | 8.65 | 1.60 |
| 20 | 14.29 | 1.42 | 11.35 | 1.51 | 9.02 | 1.60 | 7.16 | 1.73 |

Table C4. Values of a_1 , b , and λ for the different glucose concentrations c_G in PBS solutions with pH7.4 and with the different values of the ionic strength I for the investigated AAm/3-AAmPBA/BIS layer ($c_0^g = 2.23$ M).

| c_G , mM | a_1 | λ | λ | λ | λ |
|------------|-------|------------------------------|------------------------------|------------------------------|------------------------------|
| | | $I = 0.13$ M, $b = 17.13$ | $I = 0.14$ M, $b = 15.91$ | $I = 0.15$ M, $b = 14.85$ | $I = 0.16$ M, $b = 13.92$ |
| 0 | 28.84 | 1.25 | 1.24 | 1.23 | 1.21 |
| 1 | 25.98 | 1.28 | 1.26 | 1.25 | 1.23 |
| 2.5 | 22.62 | 1.31 | 1.29 | 1.28 | 1.26 |
| 5 | 18.61 | 1.36 | 1.34 | 1.33 | 1.31 |
| 10 | 13.74 | 1.47 | 1.44 | 1.43 | 1.40 |
| 15 | 10.89 | 1.57 | 1.54 | 1.53 | 1.48 |
| 20 | 9.02 | 1.66 | 1.63 | 1.60 | 1.57 |

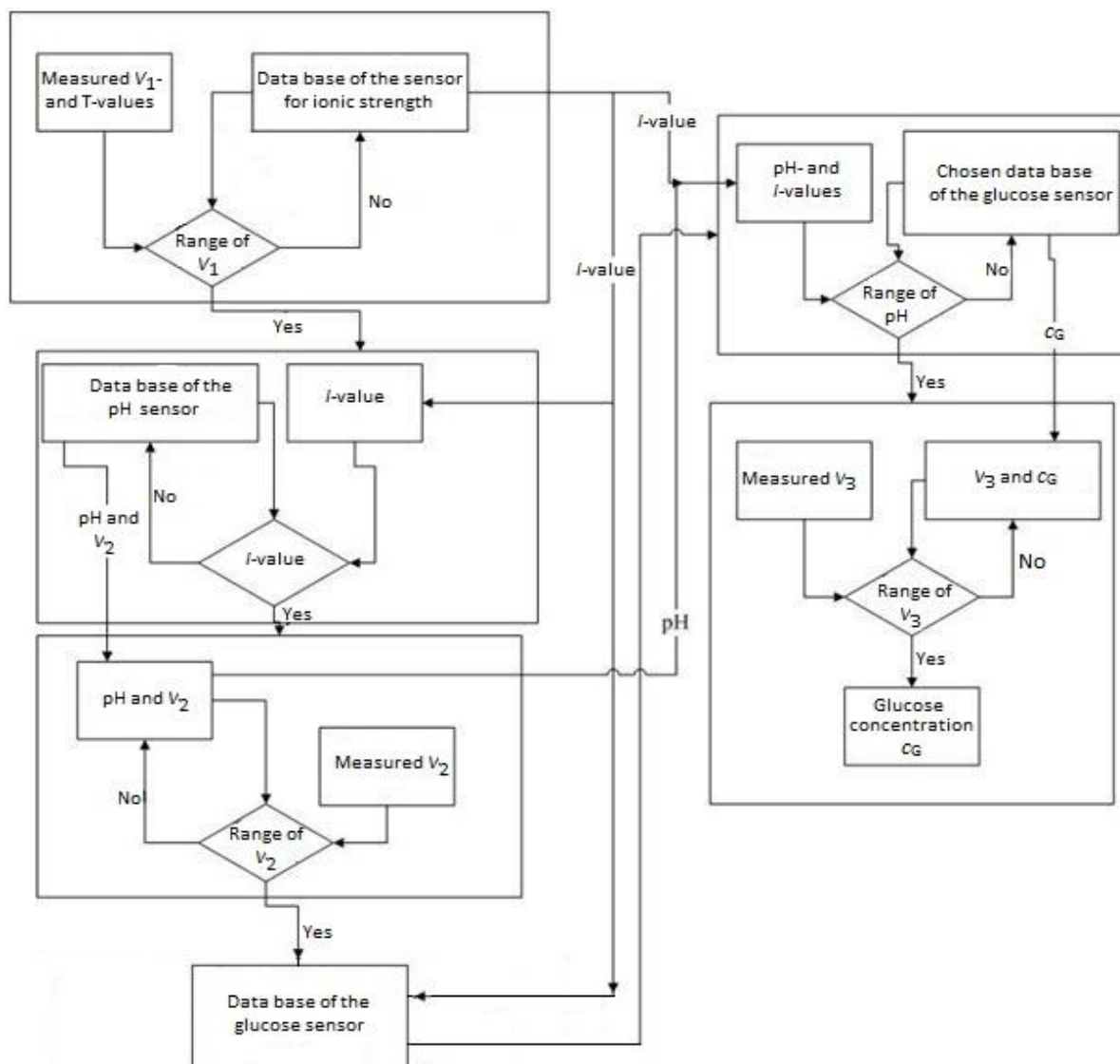
Appendix D: HPMa/DMAEMA/TEGDMA Hydrogel

Table D1. Values of a_2 , b , and λ for the different pH values of PBS solutions with the different values of the ionic strength I for the investigated HPMa/DMAEMA/TEGDMA layer ($c_0^g = 2.06$ M).

| pH | a_2 | λ | λ | λ | λ |
|-----|-------|------------------------------|------------------------------|------------------------------|------------------------------|
| | | $I = 0.13$ M, $b = 15.85$ | $I = 0.14$ M, $b = 14.72$ | $I = 0.15$ M, $b = 13.74$ | $I = 0.16$ M, $b = 12.88$ |
| 7.2 | 10 | 0.63 | 0.64 | 0.66 | 0.67 |
| 7.3 | 12.59 | 0.68 | 0.69 | 0.71 | 0.72 |
| 7.4 | 15.85 | 0.71 | 0.72 | 0.74 | 0.75 |
| 7.5 | 19.95 | 0.75 | 0.76 | 0.77 | 0.78 |

Appendix E

Figure E1. Flowchart of the programme for the calculation of the corrected values of pH and glucose concentration.



References

1. Lei, M.; Baldi, A.; Nuxoll, E.; Siegel, R.A.; Ziaie, B. A hydrogel-based implantable micromachined transponder for wireless glucose measurement. *Diabetes Technol. Ther.* **2006**, *8*, 112–122.
2. Siegel, R.A.; Gu, Y.; Lei, M.; Baldi, A.; Nuxoll, E.; Ziaie, B. Hard and soft micro- and nanofabrication: An integrated approach to hydrogel-based biosensing and drug delivery. *J. Controll. Release* **2010**, *141*, 303–313.
3. Lin, G.; Chang, S.; Hao, H.; Tathireddy, P.; Orthner, M.; Magda, J.; Solzbacher, F. Osmotic swelling pressure response of smart hydrogels suitable for chronically implantable glucose sensors. *Sens. Actuat. B* **2010**, *144*, 332–336.

4. Horkay, F.; Cho, S.H.; Tathireddy, P.; Rieth, L.; Solzbacher, F.; Magda, J. Thermodynamic analysis of the selectivity enhancement obtained by using smart hydrogels that are zwitterionic when detecting glucose with boronic acid moieties. *Sens. Actuat. B* **2011**, *160*, 1363–1371.
5. Matsumoto, A.; Kurata, T.; Shiino, D.; Kataoka, K. Swelling and shrinking kinetics of totally synthetic, glucose-responsive polymer gel bearing phenylborate derivative as a glucose-sensing moiety. *Macromolecules* **2004**, *37*, 1502–1510.
6. Koudelka, M.; Rohner-Jeanrenaud, F.; Terrettaz, J.; Bobbioni-Harsch, E.; de Rooij, N.F.; Jeanrenaud, B. *In-vivo* behaviour of hypodermically implanted microfabricated glucose sensors. *Biosens. Bioelectron.* **1991**, *6*, 31–36.
7. Koschwanez, H.E.; Reichert, W.M. *In vitro*, *in vivo* and post explantation testing of glucose-detecting biosensors: Current methods and recommendations. *Biomaterials* **2007**, *28*, 3687–3703.
8. Reach, G.; Wilson, G.S. Can continuous glucose monitoring be used for the treatment of diabetes. *Anal. Chem.* **1992**, *64*, A381–A386.
9. Orthner, M.P.; Lin, G.; Avula, M.; Buetefisch, S.; Magda, J.; Rieth, L.W.; Solzbacher, F. Hydrogel based sensor arrays (2×2) with perforated piezoresistive diaphragms for metabolic monitoring (*in-vitro*). *Sens. Actuat. B* **2010**, *145*, 807–816.
10. Guenther, M.; Gerlach, G. Hydrogels for chemical sensors. In *Hydrogel Sensors and Actuators*; Gerlach, G., Arndt, K.-F., Eds.; Springer Series on Chemical Sensors and Biosensors, Springer: Berlin Heidelberg, Germany, 2009; Volume 6, pp. 165–195.
11. Guenther, M.; Gerlach, G.; Wallmersperger, T.; Solzbacher, F.; Magda, J.J.; Lin, G.; Tathireddy, P.; Orthner, M.P. Biochemical microsensors on the basis of metabolically sensitive hydrogels. Proc. SPIE 7976, Electroactive Polymer Actuators and Devices (EAPAD) 2011, 79762D (March 28, 2011).
12. Herber, S.; Bomer, J.; Olthuis, W.; Bergveld, P.; van den Berg, A. Miniaturized carbon dioxide gas sensor based on sensing of pH-sensitive hydrogel swelling with a pressure sensor. *Biomed. Microdevices* **2005**, *7*, 197–204.
13. Hilt, J.Z.; Gupta, A.K.; Bashir, R.; Peppas, N.A. Ultrasensitive biomems sensors based on microcantilevers patterned with environmentally responsive hydrogels. *Biomed. Microdevices* **2003**, *5*, 177–184.
14. Richter, A.; Paschew, G.; Klatt, S.; Lienig, J.; Arndt, K.-F.; Adler, H.-J.P. Review on Hydrogel-based pH Sensors and Microsensors. *Sensors* **2008**, *8*, 561–581.
15. Windisch, M.; Junghans, T. Hydrogel sensors for process monitoring. *Adv. Sci. Technol.* **2013**, *77*, 71–76.
16. Buenger, D.; Topuz, F.; Groll, J. Hydrogels in sensing applications. *Prog. Polym. Sci.* **2012**, *37*, 1678–1719.
17. Muscatello, M.M.W.; Stunja, L.E.; Asher, S.A. Polymerized crystalline colloidal array sensing of high glucose concentrations. *Anal. Chem.* **2009**, *81*, 4978–4986.
18. Guenther, M.; Gerlach, G.; Wallmersperger, T.; Avula, M.N.; Cho, S.H.; Xie, X.; Devener, B.V.; Solzbacher, F.; Tathireddy, P.; Magda, J.J.; *et al.* Smart hydrogel-based biochemical microsensor array for medical diagnostics. *Adv. Sci. Technol.* **2013**, *85*, 47–52.

19. Guenther, M.; Wallmersperger, T.; Keller, K.; Gerlach, G. Swelling behaviour of functionalized hydrogels for application in chemical sensors. In *Intelligent Hydrogels*; Sadowski, G., Richtering, W., Eds.; Springer Series on Progress in Colloid and Polymer Science, Springer International Publishing, 2013; Volume 140, pp. 265–273.
20. Flory, P.J. *Principles of Polymer Chemistry*; Cornell University Press: New York, NY, USA, 1953.
21. Flory, P.J.; Rehner, J., Jr. Statistical mechanics of cross-linked polymer networks i. rubberlike elasticity. *J. Chem. Phys.* **1943**, *11*, 512–520.
22. Flory, P.J.; Rehner, J., Jr. Statistical mechanics of cross-linked polymer networks ii. Swelling. *J. Chem. Phys.* **1943**, *11*, 521–526.
23. Donnan, F.G. The theory of membrane equilibria. *Chem. Rev.* **1924**, *1*, 73–90.
24. Tanaka, T.; Fillmore, D.; Sun, S.-T.; Nishio, I.; Swislow, G.; Shah, A. Phase transition in ionic gels. *Phys. Rev. Lett.* **1980**, *45*, 1636–1639.
25. Lei, M.; Baldi, A.; Nuxoll, E.; Siegel, R.A.; Ziaie, B. Hydrogel-based microsensors for wireless chemical monitoring. *Biomed. Microdevices* **2009**, *11*, 529–538.
26. Wallmersperger, T. Modelling and simulation of the chemo-electro-mechanical behaviour. In *Hydrogel Sensors and Actuators*; Gerlach, G., Arndt, K.-F., Eds.; Springer Series on Chemical Sensors and Biosensors, Springer: Berlin Heidelberg, Germany, 2009; Volume 6, pp. 137–163.
27. Wallmersperger, T.; Ballhause, D.; Kröplin, B.; Günther, M.; Gerlach, G. Coupled multi-field formulation in space and time for the simulation of intelligent hydrogels. *J. Intel. Mater. Syst. Struct.* **2009**, *20*, 1483–1492.
28. Wallmersperger, T.; Keller, K.; Kröplin, B.; Guenther, M.; Gerlach, G. Modeling and simulation of pH-sensitive hydrogels. *Colloid. Polym. Sci.* **2011**, *289*, 535–544.
29. Wallmersperger, T.; Attaran, A.; Keller, K.; Brummund, J.; Guenther, M.; Gerlach, G. Modeling and simulation of hydrogels for the application as bending actuators. In *Intelligent Hydrogels*; Sadowski, G., Richtering, W., Eds.; Springer Series on Progress in Colloid and Polymer Science, Springer International Publishing, 2013; Volume 140, pp. 189–204.
30. Keller, K.; Wallmersperger, T.; Kröplin, B.; Guenther, M.; Gerlach, G. Modelling of temperature-sensitive polyelectrolyte gels by the use of the coupled chemo-electro-mechanical formulation. *Mech. Adv. Mater. Struct.* **2011**, *18*, 511–523.
31. 2014 General Electric Company doing business as GE Healthcare. Available online: http://www.gelifesciences.com/webapp/wcs/stores/servlet/catalog/en/GELifeSciences-de/products/AlternativeProductStructure_16220 (accessed on 29 May 2014).
32. Vo, C.D.; Kuckling, D.; Adler, H.-J.P.; Schönhoff, M. Preparation of thermosensitive nanogels by photo-cross-linking. *Colloid. Polym. Sci.* **2002**, *280*, 400–409.
33. Kuckling, D.; Hoffmann, J.; Plöner, M.; Ferse, D.; Kretschmer, K.; Adler, H.-J.P.; Arndt, K.-F.; Reichelt, R. Photo cross-linkable poly(N-isopropylacrylamide) copolymers III: micro-fabricated temperature responsive hydrogels. *Polymer* **2003**, *44*, 4455–4462.
34. Jung, D.Y.; Magda, J.J.; Han, I.S. Catalase effects on glucose-sensitive hydrogels. *Macromolecules* **2000**, *33*, 3332–3336.
35. Schulz, V.; Gerlach, G.; Günther, M.; Magda, J.J.; Solzbacher, F. Piezoresistive pH microsensors based on stimuli-sensitive polyelectrolyte hydrogels. *Techn. Messen* **2010**, *77*, 179–186.

36. Guenther, M.; Kuckling, D.; Corten, C.; Gerlach, G.; Sorber, J.; Suchaneck, G.; Arndt, K.-F. Chemical sensors based on multiresponsive block copolymer hydrogels. *Sens. Actuat. B* **2007**, *126*, 97–106.
37. *Guide to the Expression of Uncertainty in Measurement*, 1st ed.; International Organization for Standardization: Geneva, Switzerland, 1993.
38. Hoa, P.L.P.; Gerlach, G.; Suchaneck, G. Uncertainty in measurement of semiconductor piezoresistive sensors. *Microsyst. Technol.* **2003**, *9*, 210–214.
39. Ivanov, A.E.; Galaev, I.Y.; Mattiasson, B. Smart boronate-containing copolymers and gels at solid-liquid interfaces, cell, membranes, and tissues. In *Smart Polymers: Applications in Biotechnology and Biomedicine*, 2nd ed.; Galaev, I., Mattiasson, B., Eds.; CRC Press: Boca Raton, FL, USA, 2008; pp. 299–329.
40. Yan, J.; Springsteen, G.; Deeter, S.; Wang, B. The relationship among pKa, pH, and binding constants in the interactions between boronic acids and diols—It is not as simple as it appears. *Tetrahedron* **2004**, *60*, 11205–11209.
41. Miyata, T.; Uragami, T.; Nakamae, K. Biomolecule-sensitive hydrogels. *Adv. Drug Deliv. Rev.* **2002**, *54*, 79–98.
42. Arndt, K.-F.; Richter, A.; Ludwig, S.; Zimmermann, J.; Kressler, J.; Kuckling, D.; Adler, H.-J. Poly(vinyl alcohol)/poly(acrylic acid) hydrogels: FT-IR spectroscopic characterization of crosslinking reaction and work at transition point. *Acta Polym.* **1999**, *50*, 383–390.
43. Tathireddy, P.; Avula, M.; Lin, G.; Cho, S.H.; Guenther, M.; Schulz, V.; Gerlach, G.; Magda, J.; Solzbacher, F. Smart hydrogel based microsensing platform for continuous glucose monitoring. In *Merging Medical Humanism and Technology*, Proceedings of the 32nd Annual International Conference of the IEEE Engineering in Medicine and Biology Society (EMBS), Buenos Aires, Argentina, 31 August–4 September 2010; pp. 677–679.
44. Lee, M.-C.; Kabilan, S.; Hussan, A.; Yang, X.; Blyth, J.; Lowe, C.R. Glucose-sensitive holographic sensors for monitoring bacterial growth. *Anal. Chem.* **2004**, *76*, 5748–5755.
45. Schulz, V.; Zschoche, S.; Zhang, H.P.; Voit, B.; Gerlach, G. Macroporous smart hydrogels for fast-responsive piezoresistive chemical microsensors. *Procedia Eng.* **2011**, *25*, 1141–1144.